Mathematical model of evaporator for heat pump circuits

Bc. Martin Borovička[1]
Supervisors: Čížek Jan[1], Ing. Ph.D., Jean-Yves Noël[2], Ph.D.

[1] *ČVUT v Praze, Fakulta strojní, Ústav mechaniky tekutin a termodynamiky, Technická 4, 166 07 Praha 6, Česká republika*
[2] *Italia, Pordenone*

Abstract

This paper presents selected results of research project on mathematical model of evaporators for heat pump circuits. Target of this project is to model heat and mass transfer in evaporator for prescribed inlet conditions and different geometrical parameters. To obtain balance between computation time and sufficient precision of model outputs, 2D model in MATLAB is used. Model itself is unification of solvers for multiple heat and mass transfer problems - plate surface temperature, condensate film temperature, local heat and mass transfer coefficients, refrigerant temperature distribution, humid air enthalpy change. This parametric model has to be validated by experiments and then implemented into commercial CFD SW. To be able to effectively work with results from MATLAB model in CFD, approach based on POD (Proper orthogonal decomposition) and RBF (Radial basis functions) is used.

Keywords: Evaporator, heat exchanger, condensation, mathematical model

1. Introduction

Part of the research project is focused on performance of heat pump circuits, that are widely used in industry. This part is also devided into 2 parts – Mathematical model and experimental part. For the purpuse of modeling thermodynamics of HP circuit, we need to have valid mathematical models of its components. Evaporator is very important component, because it determines overall power of HP circuit, so model of evaporator will be done first.

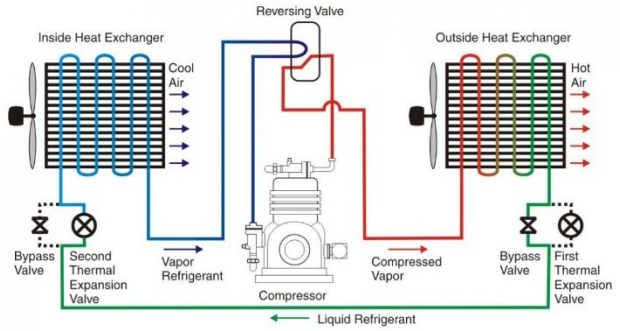

Fig. 1. Scheme of HP circuit [16]

Geometry of tube/plate evaporator that will be modeled is in following picture. Target is to model local heat and mass transfer and later on, after validation – experimental data provided by experimental part of project by measuring real evaporator, use this data in CFD model of whole HP circuit. Some data processing need to be done before implementing solution into CFD. Also user defined and user coded functions are necessary to create inside CFD to be able to effectively work with data from mathematical model.

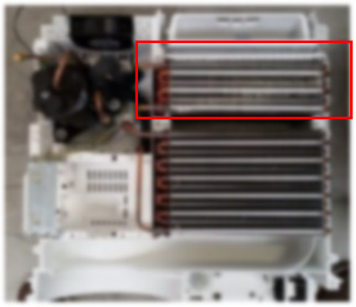

Fig. 2. Position of evaporator in HP circuit

Kontakt na autora: Martin.Borovicka@fs.cvut.cz

2. Simplifying assumptions, model type and computation region

To simplifying solution of this complex problem, we have to take these assumptions:The plate is flat.

1) For first guess, coolant temperature is constant (equal to boiling temperature) through whole evaporator. Later on some coolant temperature distribution will be solved.
2) Condansate from tubes is dropping down, not flowing down the wall.
3) Temperature of plate is constant through its thickness.
4) No heat flow from plate edges.

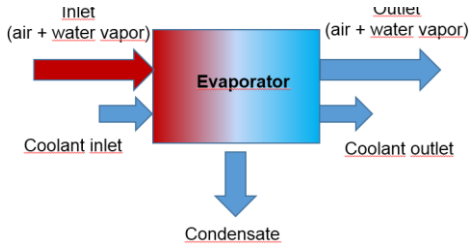

Fig. 3. Position of evaporator in tumble dryer

To obtain balance between computation time and sufficient precision of model outputs, 2D model in MATLAB is used. Another assumption is that we can solve only 1 slit between 2 plates. Overall solution of whole evaporator can be obtained by supperposition of these slits. This assumption allows us to focus only on following regions. This region si devided into rectangular mesh. This mesh has to be choosed the way that tube/plate intersections are catched precisely – high number of elements in both directions required.

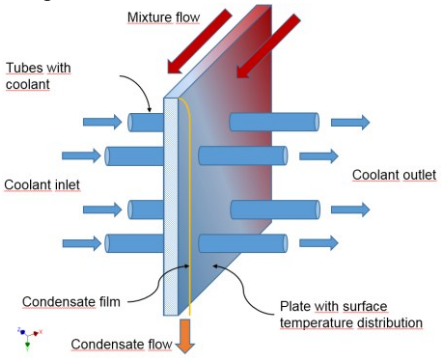

Fig. 4. Scheme of region

3. Heat and mass balance in region

Equations of heat and mass balance in 1 slit between air, film and plate/tube surface used to solve local air temperature, humidity, film temperature and mass flow.

Air/film heat halance.

$$\dot{m}_{ai,j}c_{pa}T_{gi,j} + \dot{m}_{vi,j}\left(l_{230} + c_{pv}T_{gi,j}\right) = \dot{m}_{ai+1,j}c_{pa}T_{gi+1,j} + \dot{m}_{vi+1,j}\left(l_{230} + c_{pv}T_{gi+1,j}\right) + \alpha_{gf}E_T\left(T_{gi,j} - \bar{T}_{fi,j}\right)dxdy \quad (1)$$

Film/air/surface heat balance.

$$\dot{m}_{fi,j}c_f\bar{T}_{fi,j} = \dot{m}_{fi,j+1}c_f\bar{T}_{fi,j+1} - \alpha_{gf}E_T\left(T_{gi,j} - \bar{T}_{fi,j}\right)dxdy + \alpha_{fw}\left(\bar{T}_{fi,j} - \bar{T}_{fwi,j}\right)dxdy \quad (2)$$

Coolant mass balance.

$$\dot{m}_{wi,j} = \dot{m}_{wi+1,j} \quad (3)$$

Overall mixture and film mass balance.

$$\dot{m}_{fi,j} + \dot{m}_{gi,j} = \dot{m}_{fi,j+1} + \dot{m}_{gi+1,j} \quad (4)$$

Film mass balance.

$$\dot{m}_{fi,j} + d\dot{m}_{fi,j} = \dot{m}_{fi,j+1} \quad (5)$$

Mixture mass balance.

$$\dot{m}_{gi,j} = \dot{m}_{gi+1,j} + d\dot{m}_{fi,j} \quad (6)$$

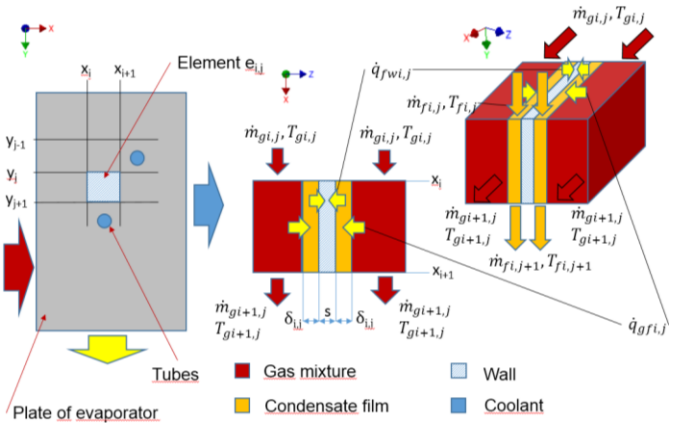

Fig. 5. Heat balance

Note:

$$\dot{m}_{gi,j} = \dot{m}_{ai,j} + \dot{m}_{vi,j};$$

$$\dot{m}_{gi+1,j} = \dot{m}_{ai,j} + \dot{m}_{vi+1,j};$$

$$\left|d\dot{m}_{vi,j}\right| = \left|d\dot{m}_{fi,j}\right|$$

Equation above form a system of differential equations in incremental form. Explicit first order Euler method is used to solve this system.

Necessary heat and mass transfer coefficients are obtained from correlation for the case of small slit and staggered tubes. These coefficients are than used to solve overal heat transfer coefficient according to following picture.

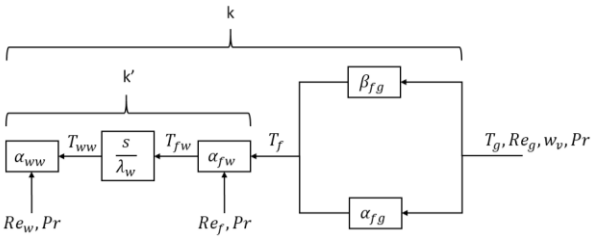

Fig. 6. Overall heat transfer coefficients

4. Viscosity effect in condensate film

Because of small thickness of film, velocity gradient can be derived as:

$$\frac{du_f}{dz} = \frac{\rho_f - \rho_g}{\mu_l} g(\delta - z) + \frac{\tau_g}{\mu_l} \tag{7}$$

After integration and implementing boundary conditions we get velocity profile:

$$u_f(z) = \frac{\rho_f - \rho_g}{\mu_l} g \left[\delta z - \frac{1}{2} z^2\right] + \frac{\tau_g}{\mu_l} z \tag{8}$$

Where ρ_f is density of condensate film, ρ_g is density of mixture and τ_g shear stress at interface between mixture and film.

Mean velocity in condensate film:

$$\bar{u}_f = \frac{1}{\delta} \int_0^{\delta} u_f(z)\, dz \tag{9}$$

Mass flow of condensate film:

$$\dot{m}_f = \rho_f \bar{u}_f \delta dx \tag{10}$$

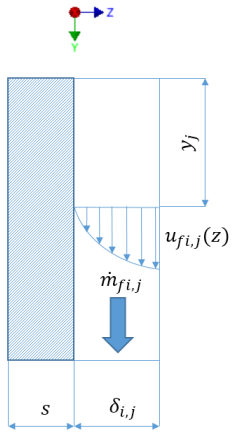

Fig. 7. Viscosity effect in condensate film

These equations can be used to solve local film thickness. This information is used to solve heat transfer through film.

5. Plate surface temperature

After taking into account simplifications, problem of plate surface temperature is reduced to 2D heat conduction problem in rectangular domain. To ensure unique solution, we need boundary conditions – we use coolant temperature in intersections of tubes and plate. As a heat load, heat flow from gas (or film) into plate will be used.

Necessary equations:

Heat flow (flux) vector:

$$\boldsymbol{q} = \begin{bmatrix} q_x \\ q_y \end{bmatrix} \tag{11}$$

Boundary normal:

$$\boldsymbol{n} = \begin{bmatrix} \boldsymbol{n_x} \\ \boldsymbol{n_y} \end{bmatrix} \tag{12}$$

Matrix of material conduction properties:

$$\boldsymbol{D} = \begin{bmatrix} \boldsymbol{k_{xx}} & \boldsymbol{0} \\ \boldsymbol{0} & \boldsymbol{k_{yy}} \end{bmatrix} \tag{13}$$

Fourier law:

$$\boldsymbol{q} = -\boldsymbol{k}\boldsymbol{\nabla}\boldsymbol{T} = \begin{bmatrix} \boldsymbol{q_x} \\ \boldsymbol{q_y} \end{bmatrix}$$

$$= -\begin{bmatrix} \boldsymbol{k_{xx}} & \boldsymbol{0} \\ \boldsymbol{0} & \boldsymbol{k_{yy}} \end{bmatrix} \begin{bmatrix} \boldsymbol{\frac{\partial T}{\partial x}} \\ \boldsymbol{\frac{\partial T}{\partial y}} \end{bmatrix} = -\boldsymbol{D}\boldsymbol{\nabla}\boldsymbol{T} \tag{14}$$

After choosing shape functions (**N**) for interpolation, weak formulation can be formulated:

$$\iint_{\Omega} \boldsymbol{B}^T t \boldsymbol{D} \boldsymbol{B} d\Omega \boldsymbol{a} =$$

$$-\oint_{\partial\Omega_q} \boldsymbol{N}^T t q_b d\partial\Omega - \oint_{\partial\Omega_T} \boldsymbol{N}^T t q_n d\partial\Omega + \iint_{\Omega} \boldsymbol{N} t Q d\Omega \tag{15}$$

Note.:

$$\boldsymbol{B} = \nabla \boldsymbol{N};$$
$$\boldsymbol{a} = [T_i];$$

Like in elasticity, stiffness matrix, boundary terms and load vector can be defined as:

The stiffness matrix:

$$\boldsymbol{K} = \iint_{\Omega} \boldsymbol{B}^T t \boldsymbol{D} \boldsymbol{B} d\Omega \tag{16}$$

Boundary terms (boundary load):

$$\boldsymbol{f}_b = -\oint_{\partial\Omega_q} \boldsymbol{N}^T t q_b d\partial\Omega - \oint_{\partial\Omega_T} \boldsymbol{N}^T t q_n d\partial\Omega \tag{17}$$

Internal load vector:

$$\boldsymbol{f}_l = \iint_{\Omega} \boldsymbol{N} t Q d\Omega \tag{18}$$

Then, we can rewrite weak formulation equations as:

$$\boldsymbol{K}\boldsymbol{a} = \boldsymbol{f}_b + \boldsymbol{f}_l = \boldsymbol{f} \tag{19}$$

This method was tried out on this example:

At the corners and in the middle of a square plate different heat of sources are placed. Blue dots represent tubes with a given temperature. Meshgrid 100x100 was used.

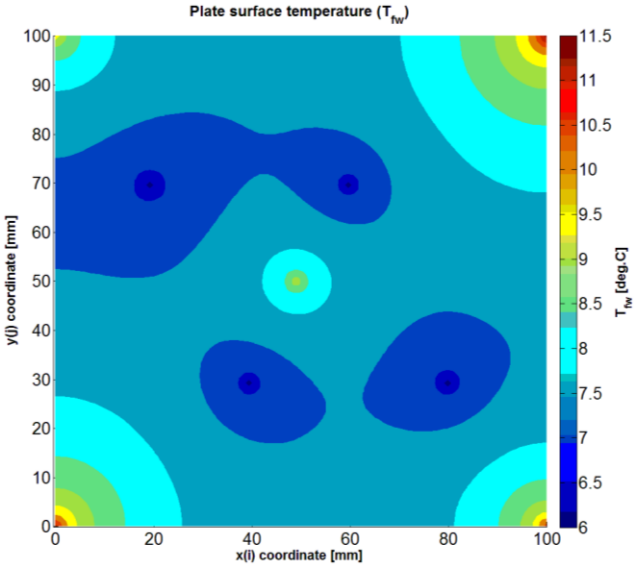

Fig. 8. Surface temperature distribution

6. Film temperature

Very important parameter, temperature of film on tubes and plates is determined from heat balance between humid air, film and plate/tube surface.

Heat balance between air, film and surface:

$$k'(T_F - T_{fw}) = d\dot{m}_f \Delta h_{23} + \alpha_{fg} E_T (T_G - T_F) \tag{20}$$

Increment of film mass flow:

$$d\dot{m}_f = m_g \beta_g ln\left(\frac{1 - \tilde{y_v}\{T_F\}}{1 - y_v}\right) \tag{21}$$

$$\phi_T = \frac{m_g \beta_g c_{pv}}{\alpha_{fg}} ln\left(\frac{1 - \tilde{y_v}\{T_F\}}{1 - y_v}\right) \tag{22}$$

Combining equations above we obtain:

$$k'(T_F - T_{fw}) = \alpha_{fg}\phi_T\left(\frac{\Delta h_{23}}{c_{pv}} + \frac{T_G - T_F}{1 - exp(-\phi_T)}\right) \tag{23}$$

Equation above is solved iteratively:

$$\rightarrow T_F^{i+1} = T_c + \frac{\alpha_{fg}\phi_T}{k'}\left(\frac{\Delta h_{23}}{c_{pv}} + \frac{T_G - T_F^i}{1 - exp(-\phi_T)}\right) \tag{24}$$

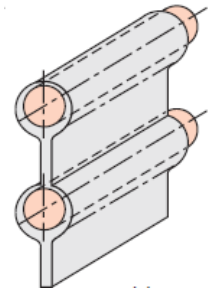

Fig. 9. Condensate film on tubes

7. Supperposition of all plates

To be able to supperpose all plates of evaporator to obtain overal solution, we need to set regions over plate, that define enthalpy change of coolant by going through this region. Based on enthalpy(temperature) change, extrapolation of solutions to other plates can be made. In general, these regions can be set by finding locations, where local heat flux is 0 or very small. Boundary of these regions are very complicated, some simplifications has to be made. Simplified region boundary is in picture bellow. Heat flow from air and film to plate and tube in this region will be used to create enthalpy change of coolant.

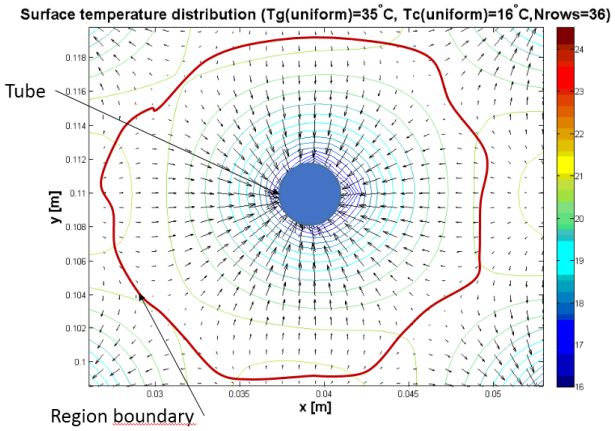

Fig. 10. Heat flow around tube-general region

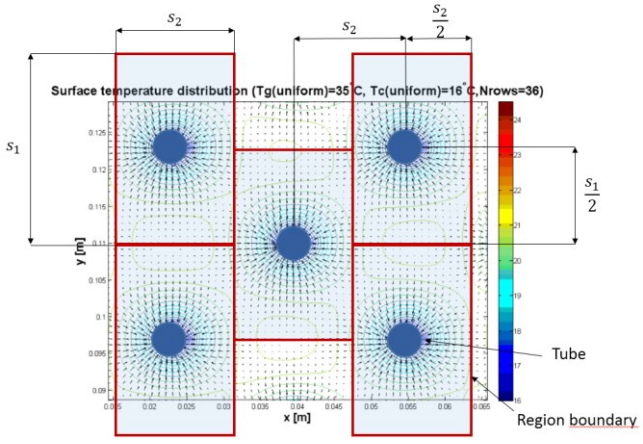

Fig. 11. Simplified regions

After setting-up regions, we can solve temperature of coolant in tube as in the case of straight tube.

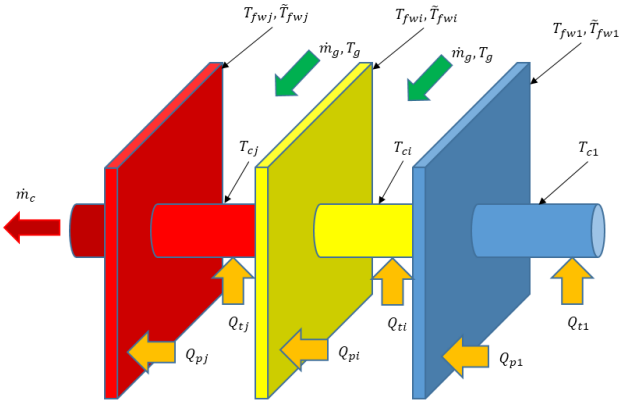

Fig. 12. Heat transfer along tube

If we assume constant distribution of heat transfer from air to coolant along one segment of tube, we can obtaion temperature distribution. Functionality of this algorithm has been tested on simplified task, where gas temperature and local heat flow is constant. Temperature distribution of refrigerant is in following picture.

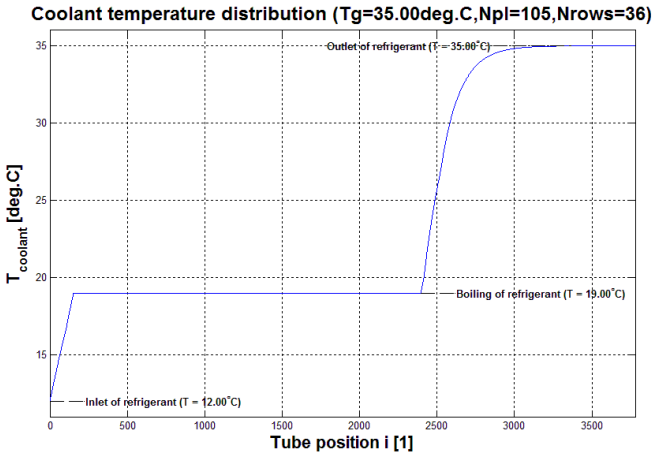

Fig. 13. Coolant temperature distribution

8. Supperposition of tube and plate heat and mass transfer

If we assume that evaporator is only composed of tubes, total heat transfer without condensation(mass transfer) can be written symbolically:

$$Q_{cond} = \tilde{\alpha}_{tube} \cdot A \cdot \left(T_g - T_f\right)_{log} \tag{25}$$

Now, if evaporator is made only from plates:

$$Q_{cond} = \tilde{\alpha}_{plate} \cdot A \cdot \left(T_g - T_f\right)_{log} \tag{26}$$

Superposing plates and tubes, total heat transfer without condensation(mass transfer) we obtain:

$$Q_{cond} = \left(R_p \cdot \tilde{\alpha}_{plate} + R_t \cdot \tilde{\alpha}_{tube}\right) \cdot A \cdot \left(T_g - T_f\right)_{log} \tag{27}$$

Superposition (effectivity) coefficients R_p, R_t has to be measured, more likely derived from measured data. Also weak dependence on Reynolds number, evaporator geometry and other parameters may be considered. Same thought can be made for mass transfer coefficient.

9. Evaporator solver scheme and convergence of solution

In following picture you can see simplified scheme of evaporator solver (subrutines: Surface temperature solver, Coolant temperature solver, (i + j) cycles to solve air and film local state).

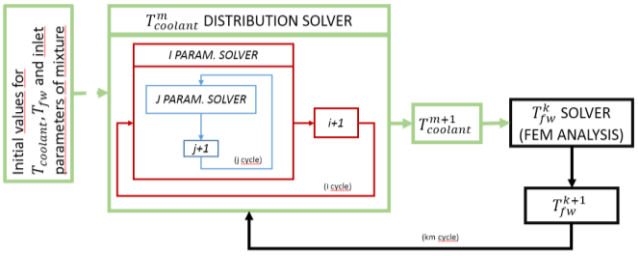

Fig. 14. Scheme of evaporator solver

Convergence of coolant temperature distribution is shown in following picture. Mean coolant temperature in collum is used. You can see, that after 6 iterations the distribution converged. Similar test was done with surface evaporator solver. Speed of convergence is similar to coolant distribution – in 5/6 iteration is solution stable. See results bellow.

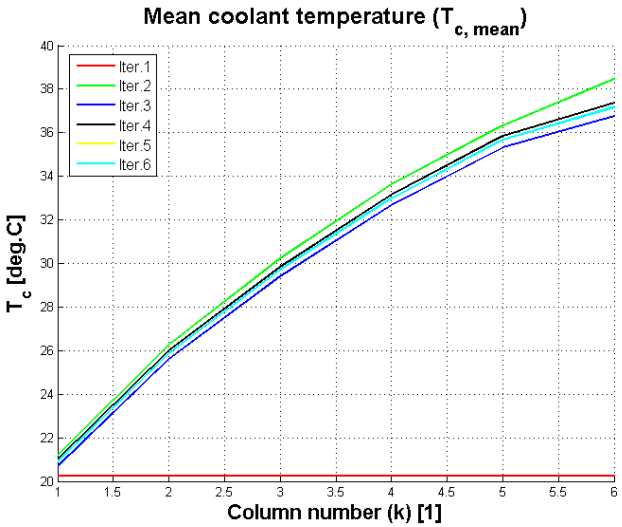

Fig. 15. Coolant temperature convergence

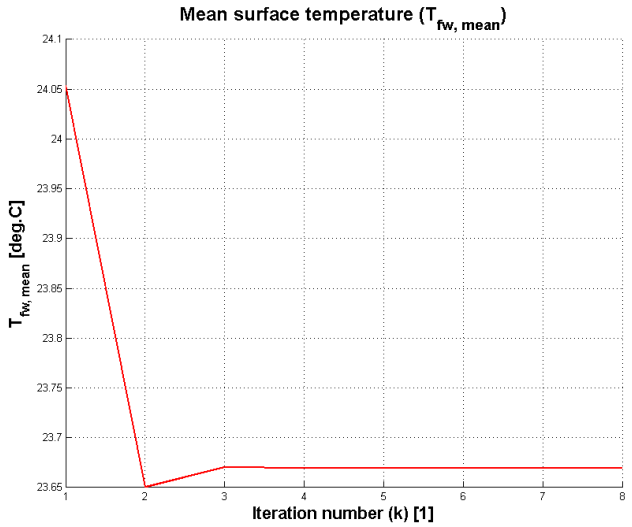

Fig. 16. Surface temperature convergence

Another test that was done is sensitivity of solution on used mesh. By increasing the number of elements in mesh. Results are shown in following picture. You can see that mesh with cca 1200 elements is sufficient.

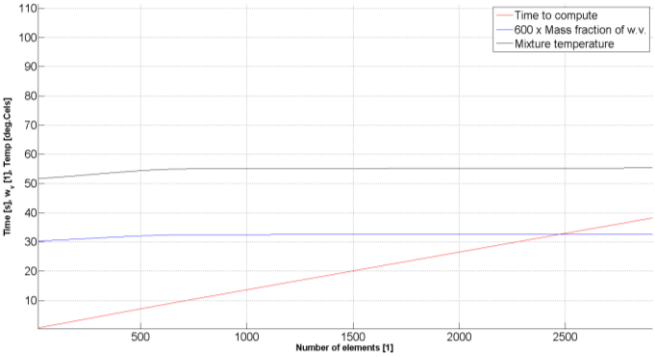

Fig. 17. Number of elements

10. POD method

POD method was discovered more than 100 years ago, but could be fully implemented only with powerfull computers.

Let's assume function $\boldsymbol{w}(\boldsymbol{x},t)$ defined over region space Ω and time region $\tau = \langle 0,T\rangle$. Function $\boldsymbol{w}$ is evaluated in many points in Ω and τ.

For example for some time t and position $\boldsymbol{x}_i$ we have $\boldsymbol{w}\big(w_1(\boldsymbol{x}_i,t), \boldsymbol{w}_2(\boldsymbol{x}_i,t), \boldsymbol{w}_2(\boldsymbol{x}_i,t),\ \ldots\big)$. Function w_1 can represent pressure, w_2-temperature, w_3-humidity etc. Region τ is not strictly time region, it can represent system parameters, initial or boundary conditions. It is suitable, to decompose function $\boldsymbol{w}$ into mean time value $\boldsymbol{u}_o$ and fluctation $\boldsymbol{u}$.

$$\boldsymbol{w}(\boldsymbol{x},t) = \boldsymbol{u}_o(\boldsymbol{x}) + \boldsymbol{u}(\boldsymbol{x},t) \tag{28}$$

Task of POD method is to decompose function $\boldsymbol{u}$ into well defined base functions $\boldsymbol{\varphi}(\boldsymbol{x})$. Base functions can be choosed as you wish, but it has to fulfill some mathematical conditions.

$$\boldsymbol{u}(\boldsymbol{x},t) = \sum_i a_i(t)\boldsymbol{\varphi}_i(\boldsymbol{x}) \tag{29}$$

$\{\boldsymbol{\varphi}_i(\boldsymbol{x})\}$ is POD base.

$\{a_t(t)\}$ are amplitudes.

To be able to decompose function $\boldsymbol{w}$ in space region Ω, we need to define average correlation tensor.

$$\boldsymbol{R}(\boldsymbol{x},\boldsymbol{x}') = \langle \boldsymbol{u}(\boldsymbol{x},t) \otimes \boldsymbol{u}(\boldsymbol{x}',t)\rangle \tag{30}$$

POD modes than can be found by solving eigenvalues for **R** tensor over space region Ω.

$$\int_\Omega \boldsymbol{R}(\boldsymbol{x},\boldsymbol{x}')\,\boldsymbol{\varphi}_i(\boldsymbol{x}')d\boldsymbol{x}' = \mu_i\boldsymbol{\varphi}_i(\boldsymbol{x}) \tag{31}$$

To be able to decompose function $\boldsymbol{w}$ in time region τ, we need to define correlation function.

$$C(t,t') = \big(\boldsymbol{u}(\boldsymbol{x},t), \boldsymbol{u}(\boldsymbol{x},t')\big)_\Omega \tag{32}$$

POD modes than can be found by solving eigenvalues for C function over time region τ.

$$\frac{1}{T}\int_0^T C(t,t')a_i(t')dt' = \lambda_i a_i(t) \tag{33}$$

Eigenvalues obtained by decomposition in space or time region are identical.

$$\mu_i = \lambda_i \tag{34}$$

Because **R** and C are defined as self-adjoint(Hermitian), functions $a_i(t)$ and functions $\boldsymbol{\varphi}_i(\boldsymbol{x})$ are orthogonal. From now on we will work only with time region decomposition of space-discrete function.

11. Method of snapshots

Discrete POD method over time region is also known as Method of snapshots. Method was proposed by Lawrence Sirovich in 1987. Let's assume N snapshots of some phenomenon in discrete time instances t_j and M space points $\boldsymbol{x}_i$.

$$\boldsymbol{w}_j = \boldsymbol{w}\big(\boldsymbol{x}_i, t_j\big);\ \ i = 1,2,\ldots,M;\ \ j = 1,2,\ldots,N$$

According to general POD method, we compute average value and fluctation,

$$\boldsymbol{u}_0 = \boldsymbol{u}_0(\boldsymbol{x}_i) = \frac{1}{N}\sum_{j=1}^{N}\boldsymbol{w}_j \tag{35}$$

$$\boldsymbol{u}_j = \boldsymbol{w}_j - \boldsymbol{u}_0 \tag{36}$$

correlation matrix:

$$C_{mn} = \frac{1}{N}\sum_{j=1}^{N}(\boldsymbol{u}_m,\boldsymbol{u}_n);\ \ m,n = 1,2,\ldots N \tag{37}$$

eigenvalues λ_k and eigenvectors $\boldsymbol{a}^k$ of correlation matrix:

$$\boldsymbol{C}\boldsymbol{a}^k = \lambda_k\boldsymbol{a}^k. \tag{38}$$

Eigenvectors $\boldsymbol{a}^k$ are composed of time amplitudes,

$$\boldsymbol{a}^k = (a_1^k, a_2^k, \dots, a_N^k)$$

POD modes are then

$$\boldsymbol{\varphi}_k(\boldsymbol{x}_i) = \frac{1}{N\lambda_k}\sum_{j=1}^{N} a_j^k \boldsymbol{u}_j \tag{39}$$

For better implementation into Matlab, we write down these equations in form of matricies.

matrix of fluctations:

$$\boldsymbol{U} = [\boldsymbol{u}_1, \boldsymbol{u}_2, \dots \boldsymbol{u}_N] \tag{40}$$

correlations matrix (W is matrix of weigths):

$$\boldsymbol{C} = \frac{1}{N}\boldsymbol{U}^T\boldsymbol{W}\boldsymbol{U} \tag{41}$$

computation of eigenvalues and eigenvectors:

$$\boldsymbol{C}\boldsymbol{a}^k = \lambda_k \boldsymbol{a}^k \tag{42}$$

normalised eigenvectors:

$$\boldsymbol{X} = \frac{1}{N}\boldsymbol{U}\left[\frac{\boldsymbol{a}^1}{\lambda_1}, \frac{\boldsymbol{a}^1}{\lambda_1}, \dots, \frac{\boldsymbol{a}^N}{\lambda_N}\right] \tag{43}$$

For highest time efficiency, it is suitable how much particular POD mode contributes on overall solution. This fact is obvious from quantity called Levell of correlation, defined:

$$L_n = \frac{\sum_{k=1}^{n}\lambda_k}{\sum_{k=1}^{N}\lambda_k};\ \ n = 1,2,\dots,N \tag{44}$$

It is obvious, that order of L_n is $0 < L_1 < L_2 < \cdots < L_N = 1$. From this fact, you can derive that not all of POD modes has to be used, because couple last modes do not contribute on overall solution at all or changes whole solution in order 10^{-14} or less. Decision, how many modes to use can be made automatically by criterium.

$$L_p < 0.99$$

Where p is index of last used POD mode. Then we can approximate solution for other set of parameters.

$\widetilde{\boldsymbol{U}} = \boldsymbol{X}\begin{bmatrix} \boldsymbol{a}^1(\boldsymbol{param}_k)\lambda_1 \\ \vdots \\ \boldsymbol{a}^N(\boldsymbol{param}_k)\lambda_N \end{bmatrix}$ - data matrix for non-simulated combination of parameters $\boldsymbol{param}_k$

$$\boldsymbol{OUTPUT}_k = \boldsymbol{OUTPUT}_{mean} + \widetilde{\boldsymbol{U}} = \boldsymbol{OUTPUT}_{mean} + \boldsymbol{X}\begin{bmatrix} \boldsymbol{a}^1(\boldsymbol{param}_k)\lambda_1 \\ \vdots \\ \boldsymbol{a}^N(\boldsymbol{param}_k)\lambda_N \end{bmatrix} \tag{45}$$

We can write this equation down symbolically:

$$"\boldsymbol{OUTPUT}_{\boldsymbol{param}_k} = \boldsymbol{OUTPUT}_{mean} + \boldsymbol{MOD}\cdot\boldsymbol{AMPLITUDE}_{\boldsymbol{param}_k}"$$

Approximation/interpolation of amplitude with respect to parameters is done with RBF.

12. RBF method

Radial basis function h is real function that depends only on distance (norm) from specified point (origin):

$$h(x) = h(\|x\|) \tag{46}$$

Any norm that satisfies mathematical properties of vector norms can be used. In this, Euclidean distance is used.

Choosed RBF kernel:

$$h_k(x) = w_k e^{-\gamma\|x-x_k\|^2} \tag{47}$$

Note.: Remember, that x is in our case a vector o parameters $\boldsymbol{param}_i$.

Then we can write down whole function:

$$h(x) = b + \sum_{k=1}^{N} h_k(x) = b + \sum_{k=1}^{N} w_k e^{-\gamma\|x-x_k\|^2} \tag{48}$$

Unknown parameters in equation above:

$b, \{w_k\}_{k=1}^N \rightarrow N+1$ unknown parameters.

But only N equations avaliable $\begin{bmatrix} x_1\ x_2 \dots x_N \end{bmatrix}^T \rightarrow \begin{bmatrix} y_1\ y_2 \dots y_N \end{bmatrix}^T$. So direct interpolation cant be used, we have to use aproximation based on least squares method.

Error function:

$$\Delta(x_k) = (h(x_k) - y_k)^2 \tag{49}$$

Total error:

$$\Delta_{tot} = \sum_{k=1}^{N}\Delta(x_k) = \sum_{k=1}^{N}\left(b + \sum_{l=1}^{N} w_l e^{-\gamma\|x_k-x_l\|^2} - y_k\right)^2 \tag{50}$$

Determination of w_k by minimizing sample error:

$$\frac{\partial}{\partial w_m}\Delta_{tot} = \frac{\partial}{\partial w_m}\sum_{k=1}^{N}\left(b + \sum_{l=1}^{N} w_l e^{-\gamma\|x_k-x_l\|^2} - y_k\right)^2 = 0 \tag{51}$$

This step generates linear system of N equations for N unknowns. But value for γ has to be choosed wisely.

If we want to minimize sample error also with respect to γ, we need to solve:

$$\frac{\partial}{\partial \gamma}\Delta_{tot} = \frac{\partial}{\partial \gamma}\sum_{k=1}^{N}\left(b + \sum_{l=1}^{N} w_l e^{-\gamma\|x_k-x_l\|^2} - y_k\right)^2 = 0 \tag{52}$$

or,

$$\frac{\partial}{\partial \gamma_m}\Delta_{tot} = \frac{\partial}{\partial \gamma_m}\sum_{k=1}^{N}\left(b + \sum_{l=1}^{N} w_l e^{-\gamma\|x_k - x_l\|^2} - y_k\right)^2 = 0 \qquad (53)$$

This generates system of N non-linear equations for N unknowns. For solving this system, gradient descent or Newton method has to be used. In following pictures you can see comparison of directly solver fields and approximated fields with POD+RBF.

Thanks to combination of POD and RBF method we are now able to reconstruct solution in any given point in parameter space and obtain required data in much shorter time than direct solution in MATLAB. This allows us to create functions, that will describe air behaviour going through evaporator and these functions can be simply implemented into CFD.

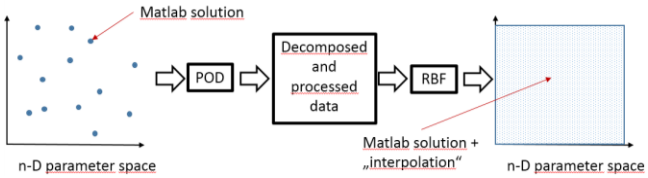

Fig. 18. Scheme of POD+RBF

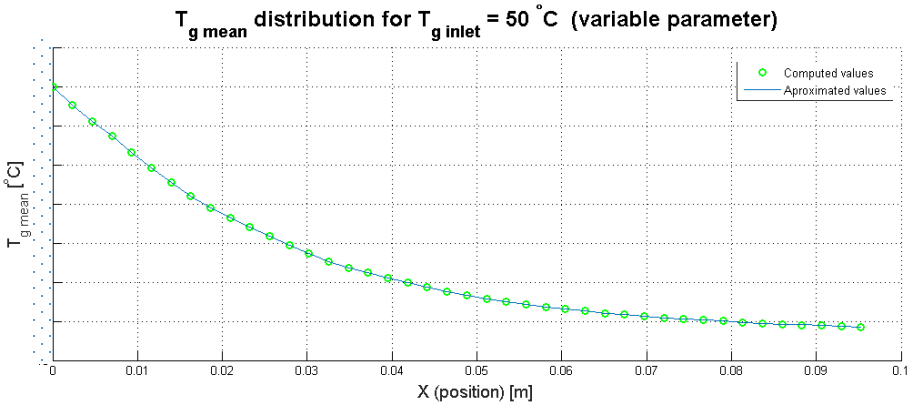

Fig. 19. Mean air temperature

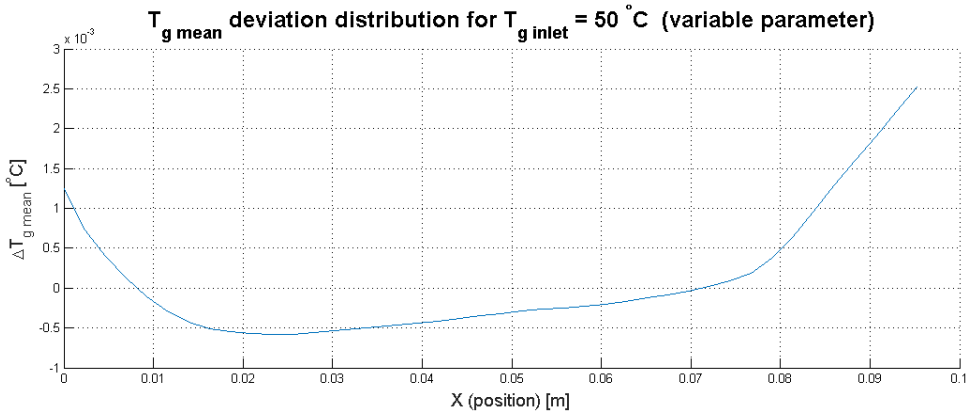

Fig. 20. Mean air temperature deviation

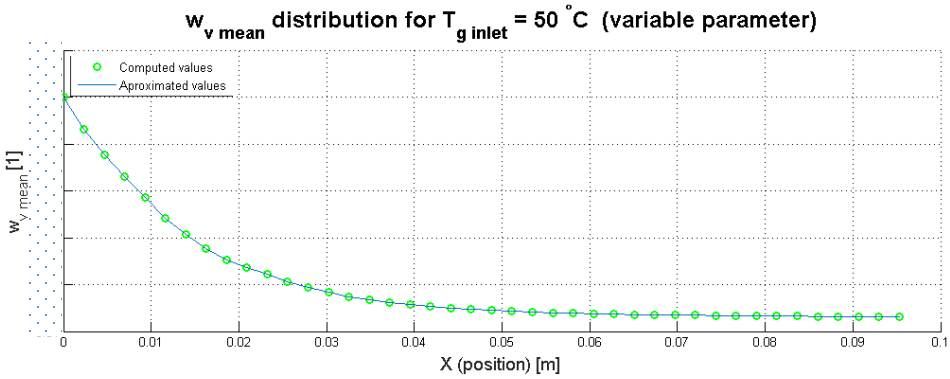

Fig. 21. Mean water vapor mass fraction distribution

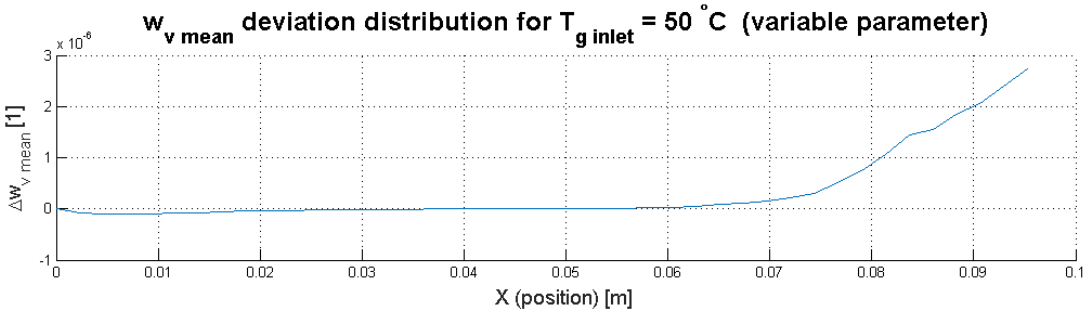

Fig. 22. Mean water vapor mass fraction distribution deviation

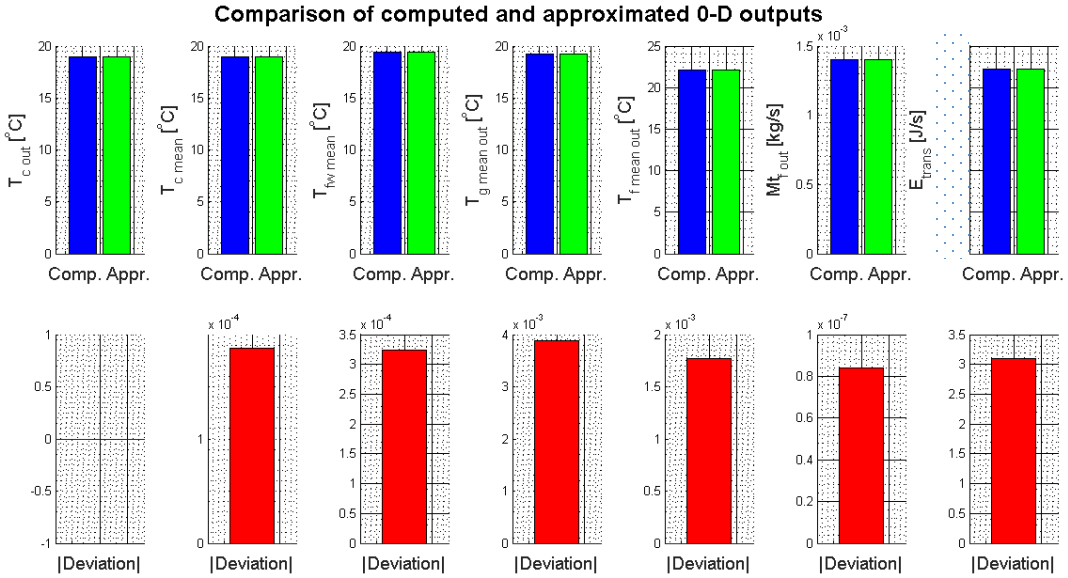

Fig. 23. 0-D outputs

13. Conclusion

Mathematical model developed during this stage of project is now beeing validated and corrected according to experimental data. At the current stage model is able to simulate humidity (even saturated state) and temperature distribution of moist air going through evaporator, based on surface temperature (FEM analysis), local coolant temperature, local heat and mass transfer on tubes and plates and local condensate film thickness. Whole model is parametric, so it is suitable for optimisation. Computation time was decreased from initial 10h - mainly by replacing loops for matrix indecies with direct matrix notation and better initial guess of surface temperature distribution to 5 min. Implementation of the model into CFD and comparison of outputs from MATLAB and CFD is in progress.

Nomenclature

$\dot{m}$	mass flow rate ($kg \cdot s^{-1}$)
p	pressure (Pa)
Q	internal heat supply ($W \cdot m^{-3}$)
q_b, q_n	boundary heat flows ($W \cdot m^{-2}$)
Ω	area of element
$\Omega_{q,T}$	boundary of element with heat or temp.condition
q	heat flux ($W \cdot m^{-2}$)
t	time (s)
μ	dynamic viscosity (Pa·s)
ρ	density (kg·m^{-3})
δ	condensate film thickness (m)
c	heat capacity ($J \cdot Kg^{-1} \cdot K^{-1}$)
α	heat transfer coefficient ($W \cdot m^{-2}K^{-1}$)
β	mass transfer coefficient ($Kg \cdot m^{-2}s^{-1}$)

Acknowledgement

Special thanks to Paolo Cescot, Ph.D., Jean-Yves Noël, Ph.D and Tomáš Hyhlík, Ing. Ph.D. for theoretical support and constructive comments.

References

[1] ŠESTÁK, J. RIEGER, F. *Přenos hybnosti, tepla a hmoty*. Praha: ČVUT, 2005. ISBN 80-01-02933-6

[2] NOŽIČKA, J. *Mechanika tekutin*. Praha: ČVUT, 2006. ISBN 80-01-02865-8

[3] NOŽIČKA, J. *Základy termomechaniky*. Praha: ČVUT, 2008. ISBN 978-80-01-04022-5

[4] ADAMEC, J. *Modelování přestupu tepla a hmoty ve filmové výplni*. Praha: ČVUT 2014. Diplomová práce, ČVUT, Fakulta strojní, Ústav mechaniky tekutin a termodynamiky.

[5] INCROPERA, F. P. *Fundamentals of heat and mass transfer*. 7th ed. USA: John Wiley& Sons, Inc., 2011. ISBN 13 978-0470-50197-9

[6] The International Association for the Properties of Water and Steam. *Properties of Ordinary Water Substance for General and Scientific Use*. Doorweth: IAPWS, 2009.

[7] JUN-DE, Li MOHAMMAD, Saraireh GRAHAM Thorpe. Condensation of vapor in the presence of non-condensable gas in condensers. *International Journal of Heat and Mass Transfer* [online]. Elsevier. May 2011, 54 (2011) 4078–4089. ISSN: 0017-9310. [14 April 2015]. Available from: http://www.elsevier.com/locate/ijhmt

[8] POOYA, M. CHAO, Z. Three-dimensional numerical model for the two-phase flow and heat transfer in condensers. *International Journal of Heat and Mass Transfer* [online]. Elsevier. November 2014, 81 (2015) 618–637. ISSN: 0017-9310. [14 April 2015]. Available from: http://www.elsevier.com/locate/ijhmt

[9] JUSSI, S. JUHA, K. ESA, V. SAMULI, S. Comparison of power plant steam condenser heat transfer models for on-line condition monitoring. *Applied Thermal Engineering* [online]. Elsevier. September 2013, 62 (2014) 37-47. ISSN: 1359-4311. [14 April 2015]. Available from: http://www.elsevier.com/locate/apthermeng

[10] J.S, Hu CHRISTOPHER, Y.H. Chao. An experimental study of the fluid flow and heat transfer characteristics in micro-condensers with slug-bubbly flow. *International journal of refrigeration* [online]. Elsevier. May 2007, 30 (2007) 1309-1318. SSN: 0140-7007. [14 April 2015]. Available from: http://www.elsevier.com/locate/ijrefrig

[11] CLÁUDIO, Melo CHRISTIAN, J.L. Hermer. A heat transfer correlation for natural draft wire-and-tube condensers. *International journal of refrigeration* [online]. Elsevier. June 2008, 32 (2009) 546–555. SSN: 0140-7007. [14 April 2015]. Available from: http://www.elsevier.com/locate/ijrefrig

[12] NYERS, Jozsef GARBAI, Laszlo NYERS, Arpad. A modified mathematical model of heat pump's condenser for analytical optimization. *Energy* [online]. Elsevier. January 2015, 80 (2015) 706e714. SSN: 0360-5442. [14 April 2015]. Available from: http://www.elsevier.com/locate/energy

[13] ARSENYEVA, Olga TOVAZHNYANSKY, Leonid KAPUSTENKO, Petro PEREVERTAYLENKO, Oleksander KHAVIN, Gennadiy. Investigation of the new corrugation pattern for low pressure plate condensers. *Applied Thermal Engineering* [online]. Elsevier. February 2011, 31 (2011) 2146-2152. ISSN: 1359-4311. [14 April 2015]. Available from: http://www.elsevier.com/locate/apthermeng

[14] TSILINGIRIS, P.T. Thermophysical and transport properties of humid air at temperature range between 0 and 100℃. *Energy conversion and managemant* [online]. Elsevier. November 2007, 49 (2008) 1098-1100. ISSN: 0196-8904. [14 April 2015]. Available from: http://www.elsevier.com/locate/enconman

[15] REZK, K. FORSBERG, J. Geometry development of the internal duct system of a heat pump tumble dryer based on fluid mechanic parameters from a CFD software. *Applied Energy* [online]. Elsevier. December 2010, 88 (2011) 1596–1605. ISSN: 0306-2619. [14 April 2015]. Available from: www.elsevier.com/ locate/apenergy

[16] Reversing valve cooling. E*corenovator* [online]. © EcoRenovator. Dostupné z: http://ecorenovator.org/forum/18881-post1066.html